Int. J. Electrochem. Sci., 10 **(2015)** 2580 - 2593

International Journal of
ELECTROCHEMICAL
SCIENCE
www.electrochemsci.org

Detection of Interferon-Gamma for Latent Tuberculosis Diagnosis Using an Immunosensor Based on CdS Quantum Dots Coupled to Magnetic Beads as Labels

Hongxing Huang[1,2], *Jiong Li*[1], *Shanshan Shi*[1], *Yuqi Yan*[1], *Mengyuan Zhang*[1], *Pengcheng Wang*[1], *Gucheng Zeng*[3], *Zhenyou Jiang*[1,2,*]

[1] Department of Microbiology and Immunology, School of Medicine, Jinan University, Guangzhou 510632, China.
[2] Guangdong Key Laboratory of Molecular Immunology and Antibody Engineering, Jinan University, Guangzhou 510632, China.
[3] Department of Microbiology, Key Laboratory for Tropical Diseases Control of the Ministry of Education, Zhongshan School of Medicine, Sun Yat-sen University, Guangzhou 510275, China.
[*]E-mail: tjzhy@jnu.edu.cn

Received: 16 November 2014 / *Accepted:* 29 December 2014 / *Published:* 19 January 2015

We describe a rapid, sensitive, and enzyme-free method to detect interferon-gamma (IFN-γ), which is associated with susceptibility to tuberculosis. A novel immunosensor using CdS quantum dots (QDs) coupled to magnetic beads (MB) as electrochemical labels has been developed for detection of IFN-γ. This sandwich-type sensor is fabricated on a glassy carbon electrode (GCE) covered with a well-ordered gold nanoparticles (AuNPs) monolayer, which offered a solid support to immobilize capture anti-human IFN-γ antibodies (Ab_1) efficiently. Then MB-QDs conjugated with detection anti-human IFN-γantibodies (Ab_2) were attached onto the AuNPs surface through a subsequent "sandwich" immunoreaction. Square wave anodic stripping voltammetry (SWASV) was carried out to quantify the metal cadmium, which indirectly reflected the amount of the analyte. Under optimum conditions, the electrochemical signal showed a linear relationship with the logarithm of IFN-γ concentration, ranging from 1 pg mL^{-1} to 500 pg mL^{-1}, and the detection limit was 0.34 pg mL^{-1}. The immunosensor showed high sensitivity, satisfactory reproducibility and reproducibility, and could be used for the detection of real sample, which provided a potential tool for latent tuberculosis diagnosis.

Keywords: interferon-gamma, quantum dots, magnetic beads, immunosensor

1. INTRODUCTION

Tuberculosis (TB) remains a global health problem with approximately one third of the world population thought to be infected with Mycobacterium tuberculosis (Mtb)[1]. Among infected individuals, only about 10% progress to active disease and the remaining 90% maintain a latent TB infection (LTBI) without clinical TB symptoms[2]. These individuals with LTBI can remain healthy for decades or, in an unknown proportion, resolve infection spontaneously but have a significantly elevated risk of developing TB during their life time[3]. Therefore, a major challenge in the treatment and management of TB remains the early identification of Mycobacterium tuberculosis infected individuals and especially those who have progressed to develop tuberculosis[4].

Current TB diagnostics, however, are in need of improvement. TB infection has been traditionally diagnosed using the Mantoux tuberculin skin test (TST), but this has been shown to be a non-specific test due to cross reactivity with other mycobacterial antigens and also because it is affected by BCG vaccination of the host[5]. Recently, commercial interferon-γ (IFN-γ) release assays (IGRAs), such as the Quanti FERON-TB Gold In-Tube test (QFT-GIT; Cellestis, Victoria, Australia)[6] and T SPOT.TB (Oxford Immunotec, Abington, UK)[7, 8], have been introduced into both clinical practice and public health policy for the diagnosis of Mtb infection to overcome the drawback of the TST. This has led to advances in the diagnosis and treatment of LTBI. In one method of detection, a sample of whole blood is stimulated with an early secretory antigenic target, such as the 6-kDa early secreted antigenic target (ESAT-6), culture filtrate protein 10 (CFP-10), and TB7.7 peptides[5,9-13]. Then, QFT-GIT can be used to detect soluble IFN-γ using an enzyme-linked immunosorbent assay (ELISA)[14]. However, the commercial T SPOT.TB kit and QFT-G kit take at least 12 h to obtain results and is highly expensive[15].

Recently, the applications based on nanoparticles (NPs) in immunoassay have attracted wide interest due to their unique optical, electronic, and mechanic properties[16]. Various NPs such as gold, silver, silica, and quantum dots (QDs) have been extensively used for ultrasensitive optical and electrochemical bioassays[17]. In particular, to enhance the sensitivities, biosensors and bioassays using electrochemical stripping analysis based on QDs have shown great potential for the detection of trace biomolecules because of their unique advantages such as nanometer size similar to proteins and versatility in surface modification with various biomolecules[18-22].

Herein, we developed an electrochemical immunoassay approach for the quantification of IFN-γ using MB-QD as labels, as shown in Scheme 2. We used a simple and facile synthetic strategy to prepare uniform-size water-soluble CdS QDs and fabricated a novel immunosensor to effectively detect IFN-γ based on the electrochemical signals. In the case of the preparation of the immunosensor, the mouse anti-human IFN-γ antibody (Ab_1) was immobilized on the glassy carbon electrode coated with a film of well-ordered AuNPs. The analytical procedure consisted of the immunoreaction of the antigen (Ag) with Ab_1, followed by binding goat anti-human IFN-γ (Ab_2) co-immobilized with QDs onto the MB, which were used as immunosensing probes for the capture of target analytes. Based on a sandwich-type immunoassay format, the formed immunocomplexes were subsequently quantified using square wave anodic stripping voltammetry (SWASV) at an in situ prepared mercury film electrode. Indeed, we could measure IFN-γ in serum in the range of 1 pg mL^{-1} to 500 pg mL^{-1} with a

detection limit of about 0.34 pg mL^{-1}. Since the reported cut-off value for LTBI is approximately 15 pg mL^{-1}[36], these results indicate that the sensitivity of the immunosensor is sufficiently high for diagnosing LTBI. The feasibility of the immunosensor for clinical applications was investigated by analyzing real sample, in comparison with the ELISA method. Consistent results were obtained by the two methods, supporting the reliability of the immunosensor. The proposed highly sensitive immunosensor provided a consideration for the diagnosis of LTBI in clinical laboratory.

2. EXPERIMENTAL SECTION

2.1 Regents and Buffers

L-Gluthathione reduced (99%), gold (III) chloride trihydrate (99.9%) and sodium borohydride (99%) 2,2'-azino-bis (3-ethylbenzthiazoline- 6-sulfonic acid), poly (diallydimethylammoniumchloride) (PDDA), Tween-20 were purchased from Sigma (USA), N-(3-Dimethylaminopropyl)-N′-ethylcarbodiimide (EDC, Sigma) and N-Hydroxysulfosuccinimide sodium salt (NHSS, Sigma) were dissolved in water immediately before use. The amino modified Magnetic Polystyrene Particles (MBs) were obtained from micromod (Germany). Phosphate buffered saline (PBS) were purchased from Boster (Wuhan, China). ELISA kits were purchased from eBioscience (USA). Monoclonal mouse anti-human IFN-γ antibody (Ab_1), detection goat anti-human IFN-γ (Ab_2) were from eBioscience (USA). Lymphocyte separation medium was purchased from Hao yang biological manufacture CO.,LTD (Tianjin, China). RPMI-1640 culture medium and fetal calf serum (FCS) were obtained from Gibco (USA). ESAT-6 and CFP-10 were synthetised by Scilight Biotechnology LLC (Beijing, China) and phytohaemagglutinin (PHA) was purchased from Beijing Dingguo Changsheng Biotechnology CO.LTD (Beijing, China). All other chemicals were of analytical grade and were used without further purification.

2.2 Instrumentation

Electrochemical experiments were performed with a CHI660E electrochemical workstation (CH Instrument Company, Shanghai, China) with a conventional three-electrode cell. A platinum wire and a saturated calomel electrode (SCE) were used as auxiliary electrode and reference electrode, respectively. Glassy carbon electrode loading different materials was used as working electrode. The structure of composites were characterized by transmission electron microscopy (TEM, Philips, Holland), scanning electron microscopy (SEM, JEOL, Japan). The structure of AuNPs was characterized by Atomic Force Microscope (AFM, Agilent Technologies, USA).

2.3 Synthesis of Glutathione protected AuNPs (GSH-AuNPs)

Glutathione protected AuNPs with diameter 20 nm were prepared by the reduction of gold salt using sodium borohydride in the presence of glutathione[23]. In brief, a quantity of 19.7 mg $HAuCl_4 \cdot 3H_2O$ and 7.7 mg of glutathione were added to a mixture of solvents, methanol (3.0 mL) and

acetic acid (0.5 mL) and dissolved by stirring for 5 min, resulting in a clear yellow solution. Sodium borohydride solution was prepared by dissolving 30 mg of $NaBH_4$ in 1.5 g of nanopure water. The $NaBH_4$ solution was added dropwise into above solution with rapid stirring. The color of $HAuCl_4$ changed from yellow to brown upon addition of $NaBH_4$ solution. Rapid stirring was continued for 2 h. The glutathione protected gold nanoparticles (GSH-AuNPs) thus formed were soluble in water. The particle solution was filtered through a 50 KDa MW cutoff, centrifuging at 3500 rpm and washed with nanopure water for 4 times, and then dissolved in 20 mM HEPES buffer at pH 8.0.

2.4 Preparation of Water-Soluble CdS QDs

L-cysteine-capped CdS-QDs were prepared according to the literature[24] with slight modifications. Briefly, $CdCl_2 2.5H_2O$ (0.158g) was dissolved in 30 mL of distilled water under stirring with a freshly prepared solution of L-cysteine (0.242g dissolved in 10 mL of water at room temperature). The mixture was injected into a freshly prepared solution of $Na_2S \cdot 9H_2O$ (0.508g in 30 mL of water), an orange–yellow solution appeared. The solution was held at room temperature for 6 h with continuous refluxing. The resultant precipitates were separated by centrifugation and washed thoroughly with absolute ethanol twice and ultrapure water three times. Then, the obtained precipitate was redispersed into water for centrifugation to collect the upper yellow solution of CdS-QDs[25].

2.5 Preparation of Magnetic Beads –QDs- Antibody Labels (MB-QD-Ab_2)

2.5.1 Preparation of QDs-coated Magnetic beads (MB-QD).

The amino modified Magnetic Polystyrene Particles (MBs) were dispersed in a mixture of 1 mL of CdS QDs (5 mg mL^{-1}) and 200 μL of freshly prepared EDC /NHSS (20 mg mL^{-1} EDC and 10 mg mL^{-1} NHSS, in 0.1 M pH 7.4 PBS)[26]. The mixed suspension was stirred at room temperature for 2 h. Unbound QDs were removed by the matrix with the aid of a magnetic device and washing with water several times. Finally, the as-prepared MB-QD nanospheres, which had the same orange color as CdS QDs itself, were obtained and dispersed in water to a final volume of 1 mL.

2.5.2 Preparation of QDs-coated Magnetic beads Immunological Labels (MB-QD-Ab_2).

To generate QDs-coated magnetic beads immunological labels, 1 mL of the above MB-QD suspension was mixed with 1 mL of Ab_2 solution (anti- human IFN-γ, 10 μg mL^{-1}, in 0.01 M pH 7.4 PBS). Subsequently, 100 μL of freshly prepared EDC (20 mg mL^{-1}, in 0.1 M pH 7.4 PBS) and 100 μL of NHSS (10 mg mL^{-1}, in 0.1 M pH 7.4 PBS) were added. After incubation at room temperature for 2 h, free antibody was removed by a magnetic device and washing with 0.01 M PBS for several times to obtain the Ab_2-modified MB-QD nanoparticles (MB-QD-Ab_2)[27, 28]. Finally, MB-QD-Ab_2 nanoparticles were redispersed in 5 mL of 1% BSA solution for 2 h, again under stirring, to block the excess amino group and nonspecific binding sites of the MB-QD-Ab_2 nanospheres. After being centrifuged and washed with PBS, the resultant MB-QD-Ab_2 nanoparticles were dispersed with 0.01

M of pH 7.4 PBS to a final volume of 2 mL and stored at 4 ℃ for later use. The whole process for construction of MB-QD-Ab_2 labels is illustrated in Scheme 1.

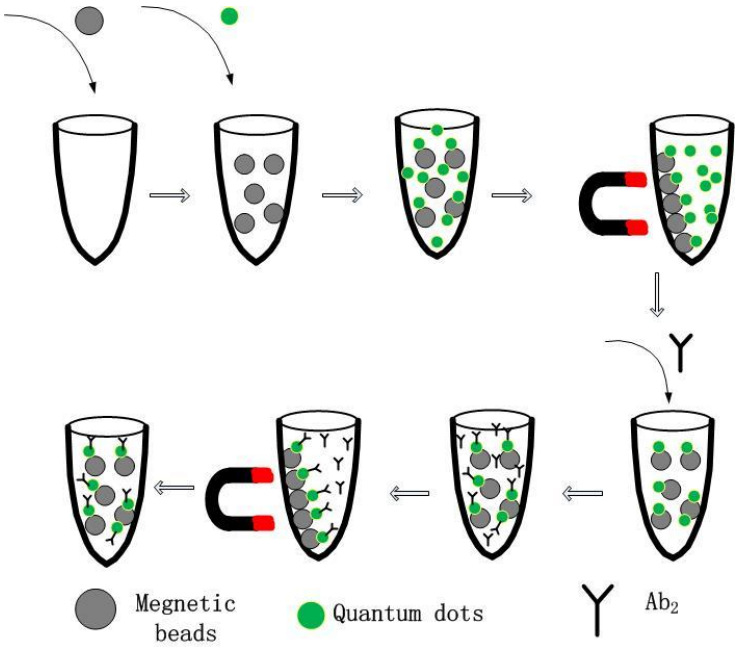

Scheme 1. Preparation of MB-QD-Ab_2 immunological labels

2.6 Fabrication of Immunosensors

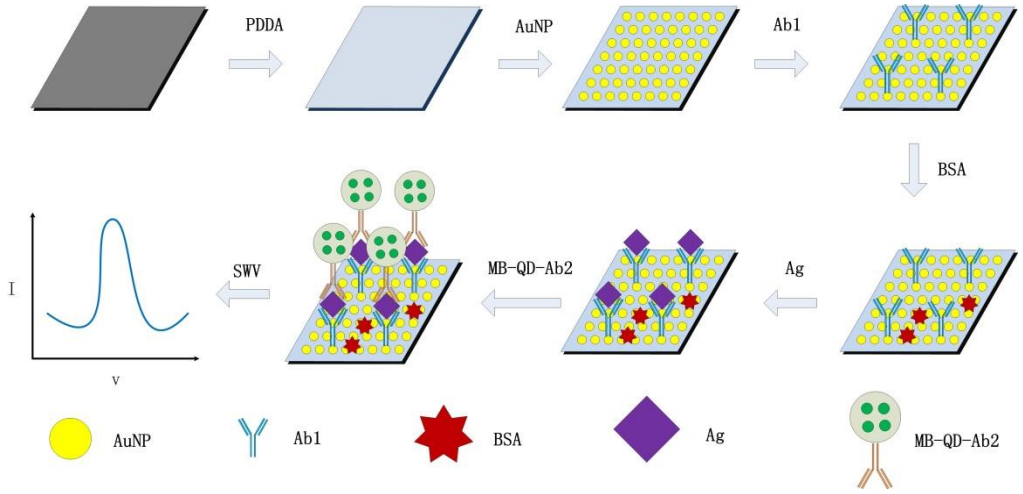

Scheme 2. Analytical procedure of electrochemical immunoassay

The glassy carbon electrode (GCE, 3 mm in diameter) was polished successively with 0.3 and 0.05 μm alumina powder, followed by successive sonication in water and ethanol. As shown in Scheme 2, 10 μL of 4 mg mL^{-1} poly (diallyldimethylammoniumchloride) (PDDA) was electro-polymerized on the freshly prepared electrode surface to form PDDA/GCE. Then 10 μL of 2 mg mL^{-1}

AuNPs was dropped on the PDDA surface and then incubated for 20 minutes to form AuNP/PDDA/GCE through electrostatic interactions between negatively charged AuNPs and positively charged PDDA. Capture antibody (Ab_1) was attached to the GSH-AuNP platform using 20 μL freshly prepared mixture of 20 mg mL^{-1} EDC and 10 mg mL^{-1} NHSS in water, washing after 10 minutes, then incubating overnight with 20 μL of 1 μg mL^{-1} primary anti- IFN-γ-antibody (Ab_1) in pH 7.4 PBS buffer[29]. Subsequently, the modified electrode was soaked in 0.01 M PBS (pH 7.4) containing 1% BSA for 1 h to block the remaining active sites and eliminate the non-specific binding effect. After washing, the obtained immunosensor incubated with 20 μL of detecting human IFN-γ samples for 1 h at 37 ℃. Next, 10 μL of MB-QD-Ab_2 was spotted onto the GCE. After an incubation of 1 h, the GCE was washed thoroughly with water to remove nonspecifically bound QDs conjugations. The procedure for fabricating the immunosensor is shown in Scheme 2.

2.7 Electrochemical Measurements

The CdS QDs remaining at the electrode surface were dissolved by the addition of 100 μL of 0.1 M HNO_3 solution[17]. The solution was transferred into 5 mL of 0.2 M acetate buffer containing 10 ppm of mercury ions (from mercuric nitrate) at pH 4.6; the amount and identity of the dissolved metal ions were determined by electrochemical stripping techniques. The square wave anodic stripping voltammetry (SWASV) was conducted with a CHI 660E electrochemical workstation. The stripping process contained a 60 s pretreatment at +0.6V and 120 s electrodeposition at -1.1 V. After that, the SWASV measurement was carried out after a 10 s rest period (without stirring) at an applied potential range of -1.0 V to -0.3 V with a potential of 4 mV, a frequency of 25 Hz, and an amplitude of 25 mV[30, 31].

2.8 Cell Preparation and Stimulation

Peripheral blood mononuclear cells (PBMCs) were isolated from heparinized venous blood under endotoxin-free conditions using Ficoll-Hypaque density gradient centrifugation. PBMC were then resuspended in RPMI-1640 medium supplemented with 100 units mL^{-1} penicillin, 100 μg mL^{-1} streptomycin and 10% fetal calf serum. PBMC were plated as 2.5×10^5 cells per well into 96 well tissue culture plate at 37 ºC, 5% CO_2 and stimulated with 10 μg mL^{-1} ESAT-6 or CFP-10 or phytohaemagglutinin (PHA) for 72h[5, 32, 33]. Cell supernatants were harvested and stored at -80 ºC for subsequent IFN- γ measurement.

2.9 ELISA Analysis

IFN-γ was measured in cell culture supernatants by ELISA according to the manufacturer's protocol.

3. RESULTS AND DISCUSSION

3.1 Atomic Force Microscope (AFM) Images of AuNPs

Figure 1 presents the AFM images of the AuNPs monolayer on smooth mica surface. The images clearly show the presence of gold nanoparticles and the monolayer was complete, homogeneous, and well ordered. PDDA was a quaternary ammonium polyelectrolyte, which was easily protonated and retained positive charge.

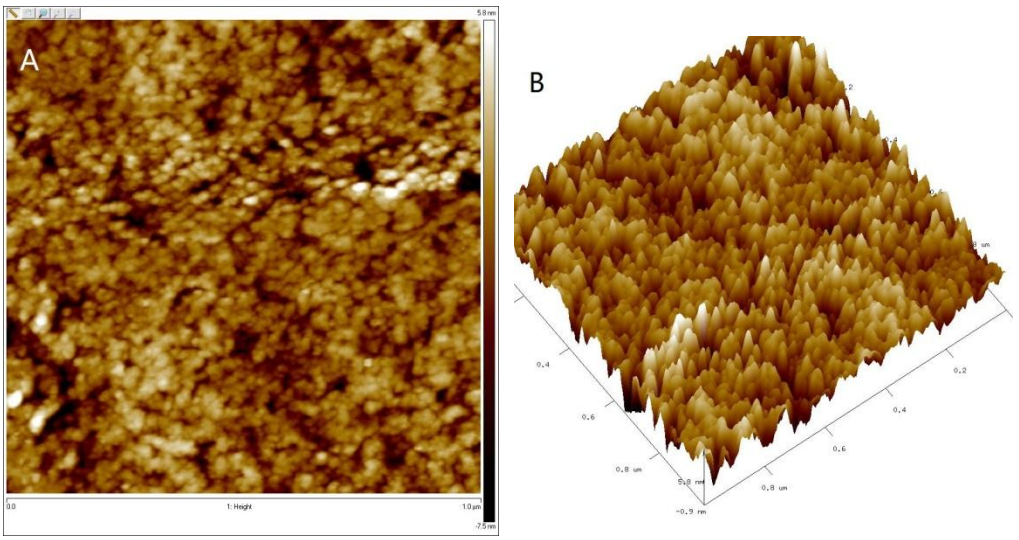

Figure 1. (A) The atomic force microscope two-dimensional image of AuNPs (B) The atomic force microscope three-dimensional image of AuNPs.

The deposition of AuNPs indicated a strong interaction between PDDA and AuNPs, which was caused by N-participation in their connection. Additionally, the connection might be promoted further by electrostatic interactions between negatively charged AuNPs and positively charged PDDA. Given that AuNPs could function as an immobilization matrix and firmly bind antibodies through ionic interactions and other interactions between AuNPs and mercapto or primary amine groups of antibodies[17], AuNP/PDDA composites appeared to offer a more homogeneous surface for antibody conjugation and subsequently antigen loading.

3.2 SEM and TEM Observations

SEM and TEM were used to investigate the formation of the MB-QD-Ab_2 composite. Figure 2 showed the typical SEM and TEM images of MB, MB-QD and the MB-QD-Ab_2 composite. SEM micrographs of the MB particles (Figure 2A) revealed distinct, uniform molecules that were spherical in shape and well separated from each other. The SEM characterization showed that MB particles are about 1μm diameter. After being coated with one layer of QDs, the surfaces of MB obtained were rougher than those of the uncoated MB, and an obvious shell on each sphere could be observed clearly,

indicating the success of the QD coating (Figure 2B). TEM images also show that the surfaces of MB-QD (Figure 2E) and MB-QD-Ab_2 (Figure 2F) were more rough than those of the MB (Figure 2D). The surfaces of MB-QD-Ab_2 were roughest among the three samples. EDC is generally utilized as a carboxyl-activating agent for amide bonding with primary amines and NHSS could enhance the coupling[34]. With EDC/NHSS crosslinking method, QDs and antibody were both immobilized on MB particles. However, amino and carboxyl group on QDs and antibody resulted in a little aggregation of nanoparticles (Figure 2B, C, F). The combined SEM and TEM data provided enough evidence of successful coating of QDs and antibody onto the surfaces of the MB.

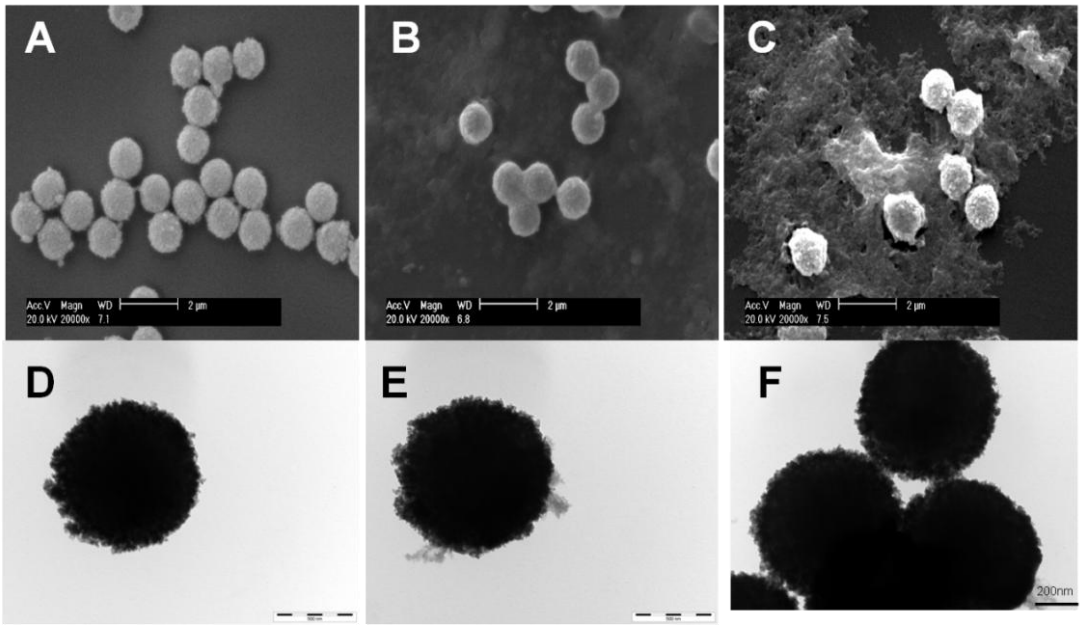

Figure 2. SEM images of (A) MB, (B) MB-QD and (C) MB-QD-Ab_2, TEM images of (D) MB, (E) MB-QD and (F) MB-QD-Ab_2

3.3 Electrochemical Characterization

Cyclic voltammetry is a simple and easy method to study the characteristics of the immunosensor at its different preparation phases. Trace a in Figure 3A shows the cyclic voltammogram obtained at a bare electrode in 10 mM PBS (pH 7.4) containing 5 mM $K_4Fe(CN)_6$, 5 mM $K_3Fe(CN)_6$ and 0.1 M KCl. The degree of modification of the sensing interface was evaluated by monitoring changes in electrochemical features of $[Fe(CN)_6]^{3-/4-}$ for a sensitive electrochemical readout[35]. As shown in Figure 3A, a couple of reversible redox peaks appeared on the bare GCE (curve a), with $[Fe(CN)6]^{3-/4-}$ as the electrochemical probe, indicating the presence of a clean and activated GCE surface. After being modified by PDDA, capable of promoting the electron transfer rate, the cyclic voltammetric (CV) signals revealed a great degree of current increase (curve b), indicating the covering of the GCE surface by PDDA. When further AuNPs were dropped on the surface of the sensor, the peak current increased (curve c) because of their ability to promote the electron transfer rate[35]. When anti-human INF-γ antibody was attached to AuNPs which anchored to

the PDDA film on the surface of the sensor, the peak current of the sensor decreased (curve d). This also indirectly indicated successful deposition of anti-human INF-γ antibody on the electrode surface. Similarly, the conductivity and reversibility were further diminished after blocking of the remaining binding sites with BSA (curve e) and modified with INF-γ antigen (curve f) and MB-QD-Ab_2 complexes (curve g).

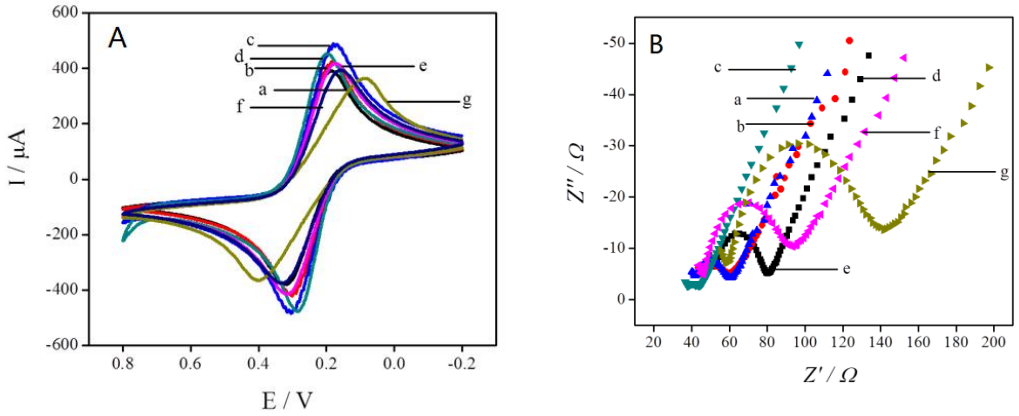

Figure 3. (A)CV of the different electrodes measured in 10 mM pH 7.4 PBS buffer solution containing 5 mM $K_4Fe(CN)_6$ and 5 mM $K_3Fe(CN)_6$; （B） EIS of the different electrodes measured in PBS (pH 7.4) : (a) GCE, (b) GCE/PDDA, (c) GCE/PDDA/AuNP, (d) GCE/PDDA/AuNP/Ab_1, (e) GCE/PDDA/AuNP/Ab_1/BSA, (f) GCE/PDDA/AuNP/Ab_1/BSA/Ag, (g) GCE/PDDA/AuNP/Ab_1/BSA/Ag/ MB-QD-Ab_2.

Electrochemical impedance spectroscopy (EIS) is an effective technique to monitor the electrode surface features. The impedance spectra include a semicircular portion and a linear portion, the semicircular portion at higher frequencies corresponds to the electron-transfer-limited process, and the linear part at lower frequencies corresponds to the diffusion process. The semicircle diameters correspond to the electron-transfer resistance[17]. We experimentally determined the EIS of the modified electrodes after the different steps. Figure 3B showed the Nyquist plots of EIS. At a bare GCE, there was a small semicircle at high frequencies and a linear part at low frequencies. When modified with PDDA on the GCE surface, a higher resistance was obtained. Because PDDA is nonconductive, its monolayer film blocks the electron transfer of redox probe $[Fe(CN)6]^{3-/4-}$ and resistance increase. When the electrode modified with AuNPs, a lower resistance was obtained because of the contribution of assembled AuNPs. Additionally, resistance significantly increased after incubation with the Ab_1, suggesting that Ab_1 were successfully immobilized on the surface and blocked the electron exchange between the redox probe and the electrode surface. The electrical resistance of the sensor increased further when the remaining active sites on working electrode were blocked with 1% BSA (curve e) as well as modified with INF-γ antigen (curve f) and MB-QD-Ab_2 complexes (curve g). The results were consistent with those of cyclic voltammetry as shown in figure 3A.

3.4 SWASV Analysis

CdS QDs loaded on immunosensor were dissolved to Cd^{2+} by HNO_3, which could be quantified by an Hg film coated glassy carbon electrode with the SWASV method[30]. Under the optimal conditions (incubation time for the antigen-antibody reaction: 60 min; 10 min for the dissolution of metal ions from the MB-QD-Ab_2 complexes), the sensitivity and dynamic range of the immunoassay were monitored by SWASV.

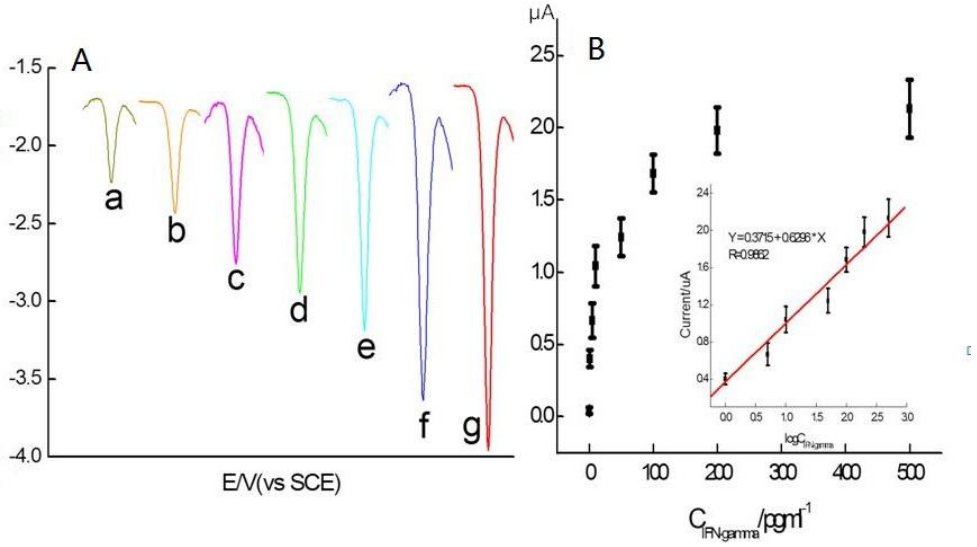

Figure 4. (A) SWASV of GCE/PDDA/AuNP/Ab_1/Ag/MB-QD-Ab_2 at IFN-γ concentration of 1 (a), 5 (b), 10 (c), 50 (d), 100 (e), 200 (f), 500 (g) pg mL^{-1}, respectively. (B) Plot of peak current obtained by dissolved PDDA/AuNP/Ab_1/Ag/MB-QD-Ab_2 versus IFN-γ concentration in incubation solution. Inset in (B): linear calibration plot (n=3).

As shown in Figure 4A, the SWASV response increased with the increase of the IFN-γ concentration from 1 to 500 pg mL^{-1}. The calibration plot (Figure 4B) displayed a good linear relationship between the peak currents and the logarithm of IFN-γ concentration in the range of 1-500 pg mL^{-1}, with a correlation coefficient of 0.9962 (n = 3). The detection limit of this method was estimated to be 0.34 pg mL^{-1} (at S/N=3). The results demonstrated that the proposed method was highly sensitive, especially for the detection of biomarkers at low levels, since the cut-off concentration for LTBI has been reported to be 15 pg ml^{-1}[36].

3.5 Application of the Immunosensor in Samples

The feasibility of the immunoassay for clinical applications was investigated by analyzing several real samples, in comparison with the ELISA method. LTBI is diagnosed when IFN-γ is detected in PBMCs culture supernatants; its presence is stimulated by the specific antigen of M. tuberculosis[37]. The serum samples were diluted 1-10 times with 0.1 mol L^{-1} pH 7.4 PBS. Figure 5 describes the correlation between the results obtained by electrochemical immunosensor assay and the

ELISA method. The relative deviations between electrochemical assay and ELISA method were in the range of -7.8 to 8.3% (Supporting information Table 1). It obviously indicates that there is no significant difference between the results given by the two methods. In addition, it was not easy to measure IFN-γ when its concentration was below the cut-off value due to the detection sensitivity of the ELISA[36]. That is, the proposed immunoassay may provide an interesting alternative tool for detection of IFN-γ in clinical laboratory.

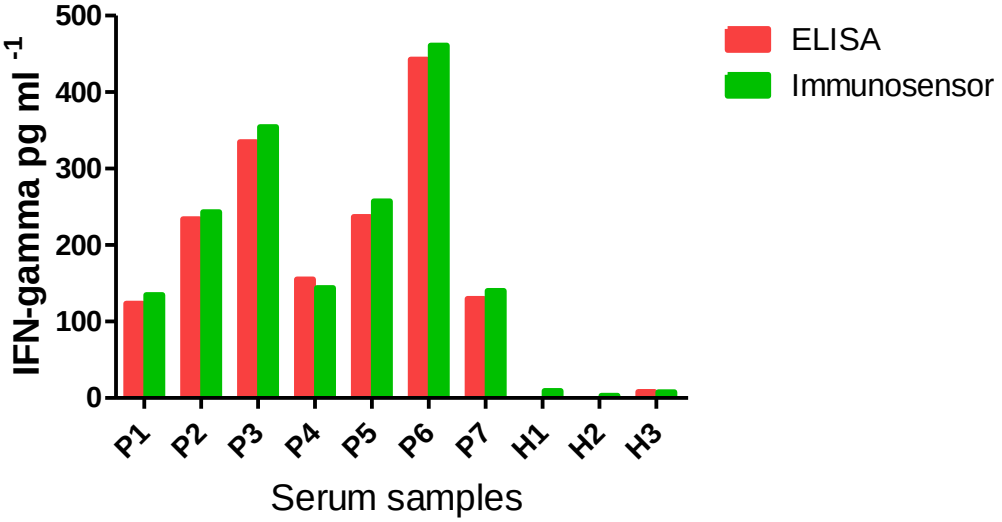

Figure 5. Comparison of serum IFN-γ using electrochemical immunosensor assay and ELISA method.(P1-P7 represent the serum samples of patients and H1-H3 represent the serum samples of healthy control)

3.6 Reproducibility, Regeneration, and Stability of the Immunosensor

The reproducibility of the immunosensor for IFN-γ was investigated with intra- and interassay precision. The intraassay precision of the biosensor was evaluated by the assay of one IFN-γ level for five replicate measurements. The interassay precision was estimated by determining one IFN-γ level, with five immunosensors made at the same substrate[27]. The intraassay and interassay variation coefficients (CVs) obtained from 100 pg mL^{-1} IFN-γ were 5.6% and 7.3% (Supporting information Figure 1), which indicated acceptable precision and good electrode-to-electrode reproducibility of the fabrication protocol described above. These results could be attributed to good monodispersion and uniformity of the gold nanoparticles.

The regeneration of the proposed immunosensor was performed using 0.1 mol L^{-1} glycine-HCl (pH 2.2) to remove the antigen and MB-QD-Ab_2 from the immunocomplex. Accordingly, after each sandwiched immunoassay, the electrode was immersed in pH 2.2 glycine-HCl for 10 min[26]. No SWASV peak current could be detected at this moment. The same immunosensor was reacted again with 100 pg mL^{-1} IFN-γ and MB-QD-Ab_2, resulted in similar SWASV responses to their original values. In repetition of these steps, SWASV intensity recovered 94% of the initial value after five

assay runs (Supporting information Figure 1). Thus, the immunosensor possessed acceptable regeneration and reuse efficiency.

Storage stability of the PDDA/AuNP/Ab_1/Ag/MB-QD-Ab_2 was also investigated by detection of SWASV after a sandwich immunoreaction at 100 pg mL^{-1} IFN-γ. When the immunosensor was stored at 4 ºC it kept its initial response for 2 weeks, which indicated that the prepared immunosensor had good storage stability and potential for practical application.

4. CONCLUSION

In this work, a novel immunoassay based on square wave anodic stripping voltammetry (SWASV) for detection of IFN-γ was developed, using MB-QD-Ab_2 nanospheres as immunological labels for signal amplification. The goal was to achieve an accurate analysis of samples using a sandwich immunoreaction. The sandwich-type immunosensor provided a convenient, low-cost, and novel method for specific and highly sensitive detection of IFN-γ. Compared with the ELISA, our sensor has a lower detection limit, and thus provides a new promising platform for clinical immunoassay. Therefore, the novel immunosensor may be applied to rapid and sensitive diagnosis of LTBI.

ACKNOWLEDGMENTS
We greatly appreciate the support of the "Twelfth Five-Year" National Science and Technology Major Project (2013ZX10003001, 2012ZX10004903), Institute of Chronic Disease Prevention and Control of Huadu District, Guangzhou, China.

References

1. S. D. Lawn and A. I. Zumla, *Lancet*, 378 (2011) 57.
2. A. O. Shakak, E. A. Khalil, A. M. Musa, K. A. Salih, A. E. Bashir, A. H. Ahmed, F. E. Idris and A. M. Elhassan, *BMC public health*, 13 (2013) 1128.
3. Y. G. Hur, P. Gorak-Stolinska, A. Ben-Smith, M. K. Lalor, S. Chaguluka, R. Dacombe, T. M. Doherty, T. H. Ottenhoff, H. M. Dockrell and A. C. Crampin, *PloS one*, 8 (2013) e79742.
4. S. Y. Kim, M. S. Park, Y. S. Kim, S. K. Kim, J. Chang, H. J. Lee, S. N. Cho and Y. A. Kang, *Scandinavian journal of immunology*, 76 (2012) 580.
5. K. I. Masood, R. Hussain, N. Rao, M. E. Rottenberg, N. Salahuddin, M. Irfan and Z. Hasan, *Journal of infection in developing countries*, 8 (2014) 59.
6. M. Frahm, N. D. Goswami, K. Owzar, E. Hecker, A. Mosher, E. Cadogan, P. Nahid, G. Ferrari and J. E. Stout, *Tuberculosis (Edinburgh, Scotland)*, 91 (2011) 250.
7. F. F. Yang, Z. Q. Tu, Y. M. Fang, Y. Li, Y. Peng, T. Dong, C. Wang, S. X. Lin, N. Y. Zhan, Z. M. Ma, Y. Z. Feng, S. Y. Tan and X. M. Lai, *Clinical and Vaccine Immunology : CVI*, 19 (2012) 401.
8. D. Goletti, S. Carrara, H. Mayanja-Kizza, J. Baseke, M. A. Mugerwa, E. Girardi and Z. Toossi, *BMC infectious diseases*, 8 (2008) 11.
9. H. Yang, H. Chen, Z. Liu, H. Ma, L. Qin, R. Jin, R. Zheng, Y. Feng, Z. Cui, J. Wang, J. Liu and Z. Hu, *PloS one*, 8 (2013) e52848.
10. H. Gao, K. Li, S. Yu and S. Xiong, *Microbiology and immunology*, 53 (2009) 541.

11. D. Silva, C. G. Ponte, M. A. Hacker and P. R. Antas, *Acta tropica*, 127 (2013) 75.
12. D. Kassa, L. Ran, W. Geberemeskel, M. Tebeje, A. Alemu, A. Selase, B. Tegbaru, K. L. Franken, A. H. Friggen, K. E. van Meijgaarden, T. H. Ottenhoff, D. Wolday, T. Messele and D. van Baarle, *Clinical and Vaccine Immunology : CVI*, 19 (2012) 1907.
13. Q. F. Sun, M. Xu, J. G. Wu, B. W. Chen, W. X. Du, J. G. Ding, X. B. Shen, C. Su, J. S. Wen and G. Z. Wang, *Medical science monitor : international medical journal of experimental and clinical research*, 19 (2013) 969.
14. F. C. Ringshausen, A. Schablon and A. Nienhaus, *Journal of Occupational Medicine and Toxicology (London, England)*, 7 (2012) 6.
15. S. H. John, J. Kenneth and A. S. Gandhe, *Biomarkers : biochemical indicators of exposure, response, and susceptibility to chemicals*, 17 (2012) 1.
16. Y. Uludag and I. E. Tothill, *Analytical chemistry*, 84 (2012) 5898
17. R. Cui, H. C. Pan, J. J. Zhu and H. Y. Chen, *Analytical chemistry*, 79 (2007) 8494.
18. K. Pinwattana, J. Wang, C. T. Lin, H. Wu, D. Du, Y. Lin and O. Chailapakul, *Biosensors & bioelectronics*, 26 (2010) 1109.
19. G. C. Fan, X. L. Ren, C. Zhu, J. R. Zhang and J. J. Zhu, *Biosensors & bioelectronics*, 59 (2014) 45.
20. S. Marin, S. Pujals, E. Giralt and A. Merkoci, *Bioconjugate chemistry*, 22 (2011) 180.
21. J. Ji, L. He, Y. Shen, P. Hu, X. Li, L. P. Jiang, J. R. Zhang, L. Li and J. J. Zhu, *Analytical chemistry*, 86 (2014) 3284.
22. M. J. Shiddiky, S. Rauf, P. H. Kithva and M. Trau, *Biosensors & bioelectronics*, 35 (2012) 251.
23. V. Mani, B. V. Chikkaveeraiah, V. Patel, J. S. Gutkind and J. F. Rusling, *ACS nano*, 3 (2009) 585.
24. M. Gui, L. Bao, Y. Xia, C. Wei, S. Zhang and C. Zhu, *Biosensors & bioelectronics*, 30 (2011) 324.
25. L. Zhang, J. H. Jiang, J. J. Luo, L. Zhang, J. Y. Cai, J. W. Teng and P. H. Yang, *Biosensors & bioelectronics*, 49 (2013) 46.
26. J. Qian, C. Zhang, X. Cao and S. Liu, *Analytical chemistry*, 82 (2010) 6422.
27. L. Yuan, X. Hua, Y. Wu, X. Pan and S. Liu, *Analytical chemistry*, 83 (2011) 6800.
28. X. Hua, Z. Zhou, L. Yuan and S. Liu, *Analytica chimica acta*, 788 (2013) 135.
29. B. S. Munge, A. L. Coffey, J. M. Doucette, B. K. Somba, R. Malhotra, V. Patel, J. S. Gutkind and J. F. Rusling, *Angewandte Chemie (International ed. in English)*, 50 (2011) 7915.
30. D. Tang, L. Hou, R. Niessner, M. Xu, Z. Gao and D. Knopp, *Biosensors & bioelectronics*, 46 (2013) 37.
31. H. Wang, J. Wang, C. Timchalk and Y. Lin, *Analytical chemistry*, 80 (2008) 8477.
32. J. Davila, L. A. McNamara and Z. Yang, *PloS one*, 7 (2012) e40882.
33. R. S. Kashyap, S. D. Shekhawat, A. R. Nayak, H. J. Purohit, G. M. Taori and H. F. Daginawala, *Clinical neurology and neurosurgery*, 115 (2013) 678.
34. Y. Zhang, J. L. Xu, Z. H. Yuan, W. Qi, Y. Y. Liu and M. C. He, *International journal of molecular sciences*, 13 (2012) 7952.
35. L. Zheng, L. Jia, B. Li, B. Situ, Q. Liu, Q. Wang and N. Gan, *Molecules*, 17 (2012) 5988.
36. J. H. Kim, Y. W. Chang, E. Bok, H. J. Kim, H. Lee, S. N. Cho, J. S. Shin and K. H. Yoo, *Biosensors & bioelectronics*, 51 (2014) 366.
37. T. Mori, M. Sakatani, F. Yamagishi, T. Takashima, Y. Kawabe, K. Nagao, E. Shigeto, N. Harada, S. Mitarai, M. Okada, K. Suzuki, Y. Inoue, K. Tsuyuguchi, Y. Sasaki, G. H. Mazurek and I. Tsuyuguchi, *American journal of respiratory and critical care medicine*, 170 (2004) 59.

Supporting information

Table 1 The concentration of IFN-γ in clinical samples measured using the Immunsensor and the ELISA.

Test	Sample/ pg ml^{-1}									
	P1	P2	P3	P4	P5	P6	P7	H1	H2	H3
ELISA	123.5	233.9	334.6	155.1	237	442.8	129.7	0	0	8
Immunosensor	134.7	243	354.5	143.9	257.4	461.2	140.1	9.3	3	7.7
Range	8.3%	3.7%	5.6%	-7.8%	7.9%	4.0%	7.4%	-	-	-3.9%

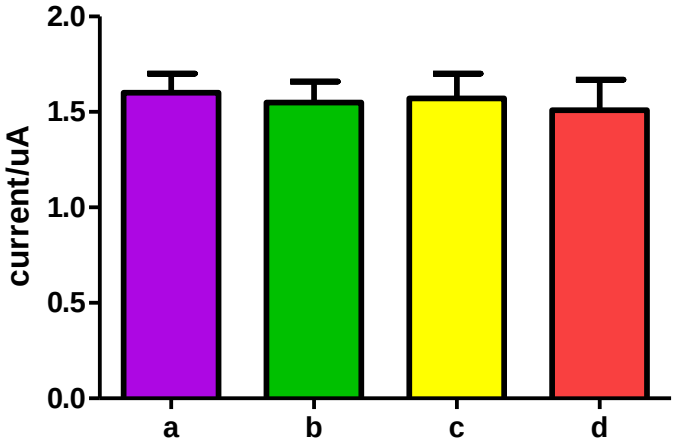

Figure 1 The reproducibility, regeneration, and stability test of the immunosensor. The current responses of the immunosensor assay with 100 pg mL^{-1} IFN-γ (a), with five immunosensors made at the same substrate at IFN-γ concentration of 100 pg mL^{-1} (b), with 100 pg mL^{-1} IFN-γ after regeneration(c), with 100 pg mL^{-1} IFN-γ after the immunosensor was stored for 2 weeks at 4 ℃(d). The error bars showed the standard deviation of five replicate measurements.